Molecular BioSystems

RSC Publishing

PAPER

View Article Online
View Journal | View Issue

# Proteomic analysis of temperature stress-responsive proteins in *Arabidopsis thaliana* rosette leaves

Cite this: *Mol. BioSyst.*, 2013, **9**, 1257

Mariapina Rocco,[a] Simona Arena,[b] Giovanni Renzone,[b] Gabriella Stefania Scippa,[c] Tonia Lomaglio,[c] Francesca Verrillo,[a] Andrea Scaloni[b] and Mauro Marra*[d]

Plants, as sessile organisms, are continuously exposed to temperature changes in the environment. Low and high temperature stresses have a great impact on agricultural productivity, since they significantly alter plant metabolism and physiology. Plant response to temperature stress is a quantitative character, being influenced by the degree of stress, time of exposure, as well as plant adaptation ability; it involves profound cellular changes at the proteomic level. We describe here the quantitative variations of the protein repertoire of *Arabidopsis thaliana* rosette leaves after exposing seedlings to either short-term cold or heat temperature stress. A proteomic approach, based on two-dimensional electrophoresis and MALDI-TOF peptide mass fingerprinting and/or nanoLC-ESI-LIT-MS/MS experiments, was used for this purpose. The comparison of the resulting proteomic maps highlighted proteins showing quantitative variations induced by temperature treatments. Thirty-eight protein spots exhibited significant quantitative changes under at least one stress condition. Identified, differentially-represented proteins belong to two main broad functional groups, namely energy production/carbon metabolism and response to abiotic and oxidative stresses. The role of the identified proteins is discussed here in relation to plant adaptation to cold or heat stresses. Our results suggest a significant overlapping of the responses to opposite temperature extremes.

Received 5th April 2013,
Accepted 10th April 2013

DOI: 10.1039/c3mb70137a

www.rsc.org/molecularbiosystems



## 1 Introduction

Plants, being in intimate contact with the environment, are continuously challenged by unfavourable conditions, such as excess/lack of water, light, nutrients or temperature extremes, all of which severely impair plant growth and reduce crop yields.[1] In order to cope with unfavourable environmental constraints, plants have evolved molecular mechanisms involving profound changes in gene expression to bring about metabolic adaptation improving fitness under stress conditions.[2] Increasing evidence from functional genomic studies suggests that information from transcriptomic data does not match necessarily the actual cellular protein complement,[3] since different modifications may affect gene products, including post-transcriptional, co-translational and degradative ones. Hence, integration of genomic data with characterization of actual protein effectors of plant stress response is necessary for a better understanding of the underlying molecular mechanisms.

Low and high temperature extremes are among the most common stresses that hamper plant growth and limit crop productivity. Response of plants to low temperatures is modulated by environmental parameters like duration and intensity of the challenge. In many plants, while a gradual exposure to moderately low temperatures for a sufficiently long time brings about an adaptation response known as acclimation,[4] which involves an extensive genetic and metabolic reprogramming, short time exposure to a more severe cold challenge triggers a rapid response whose biochemical features are only partially overlapping with those of acclimation. Molecular mechanisms underlying cold acclimation have been studied at the gene level in *Arabidospis*,[5] where key regulators, such as the transcriptional cascade ICE1-CBF[6] and HOS9 factor,[7] have been identified. In recent years, dedicated proteomic studies have been realized on *Arabidopsis*,[8–11] rice[12,13] and other species,[14] including the chilling-tolerant *Thellungiella halofila*;[15] they identified a number of cold-responsive elements, among which some stress-responsive proteins and components involved in fundamental cellular processes, such as photosynthesis, carbon assimilation, sucrose

[a] *Department of Biological and Environmental Sciences, University of Sannio, 82100 Benevento, Italy*
[b] *Proteomics & Mass Spectrometry Laboratory, ISPAAM, National Research Council, 80147 Naples, Italy*
[c] *Department of Biosciences and Territory, University of Molise, 86090 Pesche (Isernia), Italy*
[d] *Department of Biology, University of Rome "Tor Vergata", Via della Ricerca Scientifica, 100133 Rome, Italy. E-mail: Mauro.Marra@uniroma2.it*

synthesis, RNA processing, ROS detoxification and protein folding.[14] These studies have been performed both at the whole and subproteome levels,[8,16] and were mostly related to long-lasting cold treatments and to the acclimation response. Conversely, plant response to fast temperature drop has much less been investigated. Accordingly, proteomic characterization of the molecular mechanisms underlying fast cold changes is still fragmentary, relying on a limited number of papers related to various species, such as *Arabidopsis*, rice or *Thellungiella*, under different experimental conditions[8,11,15] (for a review see ref. 14). It is known that short term chilling induces rapid structural and metabolic changes, like alteration of membrane composition or synthesis of stress-protecting metabolites and/or proteins, processes that can be predominantly regulated at the post-transcriptional level.[11]

Heat stress has a severe impact on crop productivity, and the gradual increase in the ambient temperature observed in the last few decades enhances its economic impact on a global scale. Heat has an adverse effect on both vegetative growth and reproduction of plants. At the molecular level, temperature rise can have either structural effects, altering protein, membrane and cytoskeleton stability, or metabolic ones, due to alteration of enzyme activities, which in turn result in accumulation of toxic metabolites, *i.e.* reactive oxygen species (ROS).[17] Two types of heat stress response can be distinguished in plants: (i) basal thermotolerance, which is the response to a sharp temperature increase (42–45 °C) for a short time (2–6 h); (ii) acquired thermotolerance, in which plants are first exposed to moderately high temperatures or to a gradual increase, allowing them to acclimate to subsequent more severe heating.[17] Experimental evidence suggests that molecular players of the two responses are only partially shared.[18] In fact, it has been reported that some classes of chaperones, *e.g.* sHSPs or HSP70s, and APX accumulate preferentially in the acquired thermotolerance,[17] whereas the transcription factor MBF1c and catalase are key effectors in thermotolerance.[19] Proteomic studies concerning plant response to heat stress have been conducted both on model species, *i.e. Arabidopsis thaliana,*[20,21] as well as on crop species, *e.g.* rice,[20,22,23] wheat and barley.[20] Globally, these studies indicated that HSPs, as involved in protein stability, play a major role in thermotolerance; other differentially-represented components acting in redox homeostasis, carbohydrate metabolism and protein synthesis/degradation seem to be also involved in the plant response.[20–23]

In this work, we report on the main quantitative changes of the protein repertoire of *Arabidopsis thaliana* rosette leaves after exposing seedlings to short-term (6 h), low (4 °C) or high (42 °C) temperature extremes. Proteins were resolved by two-dimensional electrophoresis (2-DE) and resulting proteomic patterns were compared to control. Differently-represented components were identified by means of combined MS experiments. A significant overlap between the response to short-term cold and heat shock was originally ascertained. Functional properties of identified protein species are here discussed according to available literature data concerning response of plant to different kinds of temperature stresses.

## 2 Materials and methods

### 2.1 Plant growth and stress treatments

*Arabidopsis thaliana,* ecotype Columbia (Col-0), seedlings were grown in a growth chamber at 22 °C, 80% humidity, under a 16 h light/8 h dark cycle.[24] Three-week old plants were subjected to cold or heat stress treatments by incubating them in the dark, at 4 °C or 42 °C, respectively, for 6 and 12 h. Control plants were incubated at 21 °C for 6 and 12 h, in the dark. Leaves from stressed and control seedlings were then sampled and immediately subjected to further assays, as described below.

### 2.2 Relative electrolyte leakage measurement

The relative electrolyte leakage (REL) assay was performed under the conditions described by Yan *et al.*;[25] six biological replicates for each samples were used.

### 2.3 Protein extraction

Protein mining was performed according to the phenol extraction method,[26] with minor modifications. Briefly, plant leaves were finely powdered in liquid $N_2$ using a mortar and dried under vacuum. One gram of dried leaves was suspended in 20 mL of ice-cold extraction buffer (700 mM sucrose, 500 mM Tris-HCl, pH 7.5, 50 mM EDTA, 100 mM KCl, 2% w/v β-mercaptoethanol, 1 mM PMSF, 1% w/v PVP, 0.25% w/v CHAPS, 40 mM NaF, 1 μM okadaic acid). After addition of an equal volume of phenol saturated-500 mM Tris-HCl, pH 7.5, the mixture was stirred for 5 min in a Waring blender and then centrifuged at 10 000 × *g* for 10 min, at 4 °C. The upper phenol phase was removed and extracted once again with the extraction buffer. Proteins were precipitated from the phenol phase by addition of 5 vol of saturated ammonium acetate in methanol, at −20 °C, overnight. Precipitated proteins were centrifuged at 10 000 × *g*, for 30 min. Proteins were stored at −80 °C, until used. Three biological replicates for each treatment were analyzed, which were then subjected to an independent phenol extraction and subsequent proteomic analysis.

### 2.4 2D electrophoresis and gel image acquisition

Protein pellets were dissolved in IEF buffer (9 M urea, 4% w/v CHAPS, 0.5% v/v Triton X-100, 20 mM DTT, 1% w/v Bio-Rad carrier ampholytes pH 4–7). Protein concentration was estimated using the Bradford assay, modified according to Ramagli and Rodriguez.[27] IPG strips (17 cm, pH 4–7, Bio-Rad ReadyStrip, Bio-Rad) were rehydrated overnight with 300 μL of IEF buffer containing 300 μg of total proteins. Proteins were focused using a Protean IEF Cell (Bio-Rad) at 12 °C, by applying the following voltages: 250 V (90 min), 500 V (90 min), 1000 V (180 min) and 8000 V for a total of 52 KVh.[26] After focusing, the proteins were reduced by incubating the IPG strips with 1% w/v DTT in 10 mL of equilibration buffer (50 mM Tris-HCl, pH 8.8, 6 M urea, 30% w/v glycerol, 2% w/v SDS and a dash of bromophenol blue) for 15 min, and then alkylated with 2.5% w/v iodoacetamide in 10 mL of equilibration buffer, for 15 min. Electrophoresis in the second dimension was carried out on 12% polyacrylamide gels (180 × 240 × 1 mm) using a Protean apparatus (Bio-Rad), using electrophoresis buffer (25 mM Tris-HCl, pH 8.3, 192 mM

 

glycine and 0.1% w/v SDS), with 120 V applied for 12 h, until the dye front reached the bottom of the gel. 2-DE gels were then stained with colloidal Coomassie G250; resulting images were acquired using a GS-800 imaging system (Bio-Rad). For quantitative analysis, each sample was analyzed in technical triplicate.

### 2.5 Gel image analysis

Digitized images of Coomassie-stained gels were analyzed using the PD Quest (ver 7.4) 2-D analysis software (Bio-Rad), which allowed spot detection, landmarks identification, aligning/matching of spots within gels, quantification of matched spots and their analysis, according to manufacturer's instructions. Manual inspection of the spots was performed to verify the accuracy of automatic gel matching; any errors in the automatic procedure were manually corrected prior to final data analysis. The spot volume was used as the analysis parameter for quantifying protein expression. The protein spot volume was normalized to the spot volume of the entire gel (*i.e.*, of all the protein spots). Fold-changes in protein spot levels were calculated between spot volumes in the treated group relative to that in the control one. Statistically significant changes in protein expression were determined using two sequential data analysis criteria. First, a protein spot has to be present in all gels for each sample to be included in the analysis. Next, statistically significant changes in protein expression were determined using the distribution of fold-change values in the data. Spots were determined to be statistically significant (by Student's $t$ test) if the difference between the average intensity of a specific protein spot in the control and treated plants (three technical replicates of three biological samples) was greater than one standard deviation of the spot intensities for both groups. An absolute two-fold change in normalized spot densities was considered indicative of a differentially modified protein; thus, values $\geq 2$ or $\leq 0.5$ were associated with increased or decreased protein amounts after treatment, respectively.

### 2.6 Protein digestion and MS analysis

Spots from 2-DE were manually excised from gels, triturated and washed with water. Proteins were *in-gel* reduced, *S*-alkylated and digested with trypsin, as previously reported.[28] Protein digests were subjected to a desalting/concentration step on microZipTipC18 pipette tips (Millipore Corp., Bedford, MA, USA) before MALDI-TOF peptide mass fingerprinting (PMF) and/or nanoLC-ESI-LIT-MS/MS analysis.

During MALDI-TOF PMF experiments, peptide mixtures were loaded on the instrument target together with α-cyano-4-hydroxycinnamic acid as a matrix, using the dried droplet technique. Samples were analysed using a Voyager-DE PRO mass spectrometer (Applied Biosystems, USA). Peptide mass spectra were acquired in reflectron mode; internal mass calibration was performed with peptides derived from trypsin autoproteolysis. Data were elaborated using the DataExplorer 5.1 software (Applied Biosystems). PSD fragment ion spectral analysis of the most abundant mass signal within each MALDI-TOF mass spectrum was performed as previously reported.[29] Peptide mixtures were eventually analyzed by nanoLC-ESI-LIT-MS/MS using a LTQ XL mass spectrometer (ThermoFinnigan, USA) equipped with a Proxeon nanospray source connected to an Easy-nanoLC (Proxeon, Denmark).[30] Peptide mixtures were separated on an Easy $C_{18}$ column (100 × 0.075 mm, 3 μm) (Proxeon) using a gradient of acetonitrile containing 0.1% formic acid in aqueous 0.1% formic acid; acetonitrile ramped from 5% to 35% over 15 min and from 35% to 95% over 2 min, at a flow rate of 300 nL $min^{-1}$. Spectra were acquired in the range $m/z$ 400–2000. Acquisition was controlled by a data-dependent product ion scanning procedure over the three most abundant ions, enabling dynamic exclusion (repeat count 2 and exclusion duration 1 min). The mass isolation window and collision energy were set to $m/z$ 3 and 35%, respectively.

### 2.7 Protein identification

MASCOT software package version 2.2.06 (Matrix Science, UK)[31] was used to identify spots unambiguously from an updated plant non-redundant sequence database (UniProt 2009/05/03). MALDI-TOF PMF data were searched using a mass tolerance value of 40–80 ppm, trypsin as a proteolytic enzyme, a missed cleavage maximum value of 2 and Cys carbamidomethylation and Met oxidation as fixed and variable modification, respectively. NanoLC-ESI-LIT-MS/MS data were searched using a mass tolerance value of 2 Da for precursor ions and 0.8 Da for MS/MS fragments, trypsin as a proteolytic enzyme, a missed cleavage maximum value of 2 and Cys carbamidomethylation and Met oxidation as fixed and variable modification, respectively. MALDI-TOF PMF candidates with a cumulative MASCOT score > 83, which were also confirmed by PSD data (data not shown), or nanoLC-ESI-LIT-MS/MS candidates with at least 2 assigned peptides with an individual MASCOT score > 25, both corresponding to $p < 0.05$ for a significant identification, were further evaluated by the comparison with their calculated $M_r$ and p$I$ values, using the experimental ones obtained from 2-DE.

## 3 Results and discussion

### 3.1 Effect of temperature stresses on cell membranes

Since cold and heat short-term treatments did not result in any evident alteration of plant growth or phenotype, we evaluated the increase of ion permeability of cell membranes, which is considered as an indicator of damage induced by different stresses including cold[15] and heat[23] ones. In particular, we measured the relative electrolyte leakage of *Arabidopsis* rosette leaves incubated at 4 °C or at 42 °C, for 6 and 12 h. After 6 h, both temperature treatments altered cell membrane ion permeability, as witnessed by the slight increase of REL we observed over control values, which further raised after 12 h (Fig. 1). These results indicated that opposite temperature challenges for the same periods of time effectively determined stress conditions in *Arabidopsis* leaves, thereby eliciting cellular response mechanisms suitable to be investigated by proteomic analysis. Our results were fairly in accordance with previous reports on other plant species, which indicated a relatively low level of membrane damage in response to short-term cold[12,15]

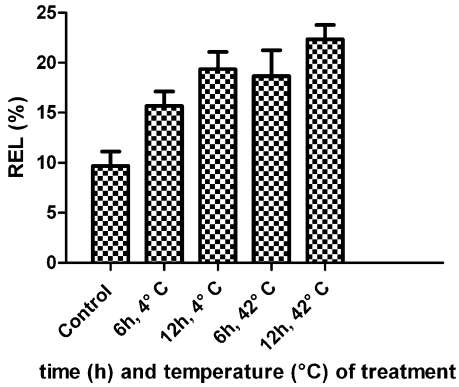


**Fig. 1** Relative electrolyte leakage (REL) from rosette leaves of *Arabidopsis thaliana*. Three-week-old seedlings were treated at 4 °C or 42 °C, for 6 or 12 h, and then REL was measured. Mean values ± SD from six replicates are reported. Control refers to plants incubated at 21 °C for 6 h, in the dark; identical data were obtained for control plants incubated at 21 °C for 12 h, in the dark.



or heat challenge.[21–23] Similarly to these studies, a higher sensitivity of *Arabidopsis* cell membranes to short-term heat than cold stress was observed; this phenomenon was associated with the capacity of heat stress to induce ROS production more rapidly than the cold one, subsequently determining a higher lipid peroxidation and final damage to membranes.[23]

### 3.2 Proteomic analysis of *Arabidopsis* leaf proteins under cold and heat shock

A proteomic approach was then used in order to identify proteins whose abundance changed upon short term heat or cold stress of *Arabidopsis thaliana* rosette leaves. Total proteins were extracted from leaves of plants incubated at 4 °C (cold shock) or 42 °C (heat shock) for 6 h, and the corresponding control, and then resolved by 2D electrophoresis, within the p*I* range 4–7 and mass range 10–150 kDa; representative 2D gels are shown in Fig. 2. To ascertain quantitative changes in relative spot volumes for temperature-treated leaves compared to control, colloidal Coomassie-stained gels were subjected to comparative software-assisted image analysis. Average proteomic maps showed 296 ± 25 (cold stress), 302 ± 31 (heat stress) and 267 ± 28 (control) spots. Statistical evaluation of relative spot volumes allowed us to detect spots significantly varying ($p < 0.05$) in abundance in challenged leaves, as compared to control ones. In total, 38 protein spots were detected, whose abundance changed in leaves in response to cold or heat shock. Among that, 28 resulted from cold-stressed *vs.* control comparison, while 37 resulted from heat-stressed *vs.* control comparison; they represented 9% and 11% of the protein spots resolved within the leave reference gel, respectively. All spots showed variably-represented quantitative levels among samples, except two that were present only in control. These figures are comparable to those of most proteomic studies concerning the effect of short and even long-term cold or heat stress in *Arabidopsis* and other species, based on 2D gel resolution of cellular protein complement (for a review see ref. 14). Hence, probably, the relatively low number of differential proteins detected is not related to

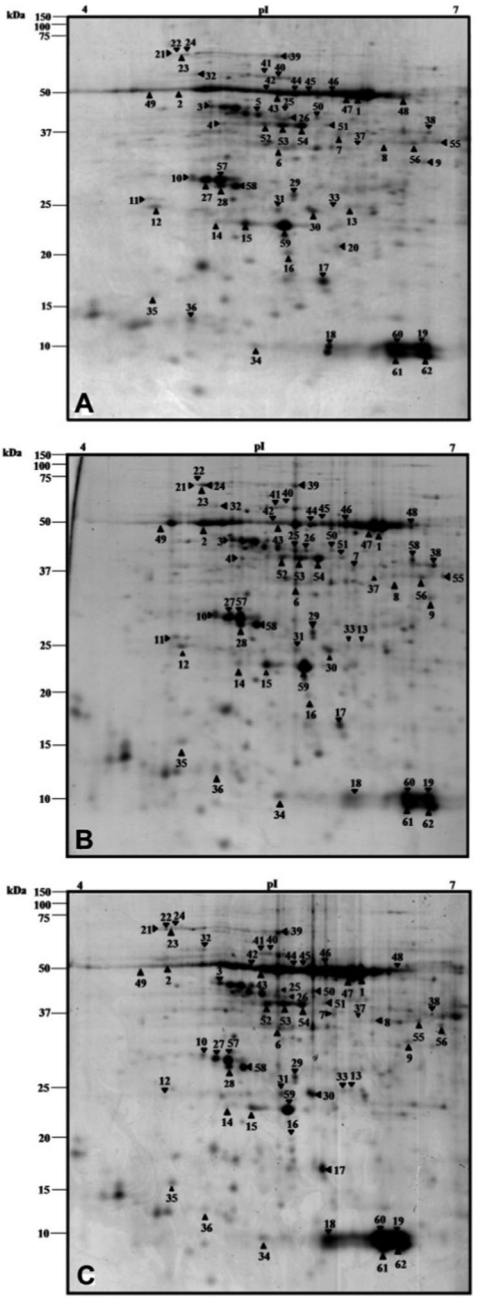


**Fig. 2** Two-dimensional electrophoresis maps of total protein extracts from *Arabidopsis* rosette leaves. Panel A, plants treated at 21 °C, for 6 h (control); panel B, plants treated at 4 °C, for 6 h (cold shock); panel C, plants treated at 42 °C, for 6 h (heat shock). Differentially represented (38 in number) or invariant (24 in number) protein spots identified are numbered. Proteins were separated over the p*I* range 4–7 in the first dimension and on 12% SDS–polyacrylamide gels in the second dimension. Gels were stained with colloidal Coomassie G250.

the low level of cellular damage induced under short time stress, but rather due to the intrinsic limitations of 2D gel-based proteomics, in which most abundant proteins and/or soluble ones are preferentially identified.

Differential spots were excised from gels, trypsinolyzed and subjected to MS analysis for further protein identification assignment. Twenty-two positive identification results derived

 

**Table 1** Proteins with changed or constant expression levels in *Arabidopsis thaliana* rosette leaves after cold or heat shock challenge. Spot number, protein name, accession number (UniProt and TAIR), identification (ID) method, sequence coverage, number of observed peptides, identification score, theoretical and experimental p*I* and $M_r$ values, and fold change in temperature-treated *vs.* control plants are listed. PMF, peptide mass fingerprinting; TMS, tandem mass spectrometry, N.d., not detectable in temperature-stressed samples. – refers to values comprised between 0.6 and 1.9 fold changes

| Spot | Protein name | UniProt accession | TAIR accession | ID method | Sequence cov% (peptides) | ID score | Theor. $M_r$ (kDa)/p*I* | Exp. $M_r$ (kDa)/p*I* | Relative fold change *vs.* control | |
|---|---|---|---|---|---|---|---|---|---|---|
| | | | | | | | | | Cold | Heat |
| 1 | Ribulose bisphosphate carboxylase large chain | O03042 | AtCg00490 | PMF | 60 (31) | 233 | 52.7/5.88 | 51.1/5.92 | 2.0 | 0.3 |
| 2 | Ribulose bisphosphate carboxylase large chain | O03042 | AtCg00490 | PMF | 60 (31) | 233 | 52.7/5.88 | 52.1/4.91 | 4.8 | 0.3 |
| 3 | Ribulose bisphosphate carboxylase/oxygenase activase, chloroplastic | P10896-1 | At2g39730 | PMF | 47 (17) | 209 | 46.2/5.09 | 44.4/5.10 | 2.2 | 4.3 |
| 4 | Magnesium-chelatase subunit ChlI-1, chloroplastic | P16127 | At4g18480 | PMF | 34 (10) | 174 | 39.9/5.05 | 39.0/5.17 | 2.0 | N.d. |
| 5 | Glutamine synthetase, chloroplastic/ mitochondrial | Q43127 | At5g35630 | PMF | 49 (19) | 220 | 42.4/5.28 | 42.4/5.36 | N.d. | N.d. |
| | Elongation factor Tu, chloroplastic | P17745 | At4g20360 | PMF | 36 (13) | 154 | 44.7/5.31 | | | |
| 6 | Probable fructose-bisphosphate aldolase 2, chloroplastic | Q944G9 | At4g38970 | PMF | 48 (12) | 203 | 38.0/5.36 | 35.3/5.51 | 2.1 | 0.4 |
| 7 | ATP synthase gamma chain 1, chloroplastic | Q01908 | At4g04640 | TMS | 26 (9) | 409 | 35.7/6.16 | 37.2/5.81 | 2.1 | 0.4 |
| 8 | Chloroplast stem-loop binding protein of 41 kDa, chloroplastic | Q9LYA9 | At3g63140 | TMS | 21 (6) | 340 | 36.3/6.04 | 35.5/6.23 | 0.5 | 0.3 |
| 9 | Photosystem I reaction center subunit II-2, chloroplastic | Q9SA56 | At1g03130 | TMS | 49 (19) | 585 | 17.7/9.30 | 30.2/6.51 | — | 0.4 |
| 10 | Soluble inorganic pyrophosphatase 1, chloroplastic | Q9LXC9 | At5g09650 | PMF | 26 (8) | 157 | 33.4/5.72 | 26.8/4.98 | — | 0.4 |
| 11 | 29 kDa ribonucleoprotein, chloroplastic | Q43349 | At3g53460 | TMS | 40 (11) | 698 | 29.2/4.76 | 25.8/4.74 | 2.1 | N.d. |
| 12 | 29 kDa ribonucleoprotein, chloroplastic | Q43349 | At3g53460 | TMS | 40 (11) | 656 | 29.2/4.76 | 25.0/4.78 | — | 0.1 |
| 13 | Photosystem I reaction center subunit II-2, chloroplastic | Q9SA56 | At1g03130 | TMS | 44 (9) | 577 | 17.7/9.30 | 25.0/5.90 | — | 0.4 |
| 14 | Oxygen-evolving enhancer protein 2–1, chloroplastic | Q42029 | At1g06680 | PMF | 48 (7) | 129 | 20.2/5.27 | 22.0/5.13 | 3.4 | 0.5 |
| 15 | Oxygen-evolving enhancer protein 2–1, chloroplastic | Q42029 | At1g06680 | PMF | 87 (11) | 148 | 20.2/5.27 | 22.0/5.34 | — | 0.3 |
| 16 | Germin-like protein subfamily 3 member 3 | P94072 | At5g20630 | TMS | 14 (7) | 255 | 19.5/5.84 | 20.7/5.55 | 0.5 | 0.1 |
| 17 | Peptidyl-prolyl *cis–trans* isomerase CYP20-3, chloroplastic | P34791 | At3g62030 | PMF | 75 (15) | 199 | 19.9/5.47 | 19.1/5.70 | 0.5 | 0.5 |
| 18 | Ribulose bisphosphate carboxylase small chain 2B, chloroplastic | P10797 | At5g38420 | PMF | 93 (20) | 179 | 14.8/5.71 | 10.5/5.75 | 2.1 | 0.5 |
| 19 | Ribulose bisphosphate carboxylase small chain 2B, chloroplastic | P10797 | At5g38420 | PMF | 93 (20) | 179 | 14.8/5.71 | 10.5/6.51 | 2.3 | 0.5 |
| 20 | Outer membrane lipoprotein Blc | Q9FGT8 | At5g58070 | TMS | 23 (4) | 391 | 21.4/5.98 | 21.0/5.81 | N.d. | N.d. |
| | Ribulose bisphosphate carboxylase large chain (fragment) | O03042 | AtCg00490 | PMF | 60 (31) | 233 | 52.7/5.88 | | | |
| 21 | Heat shock 70 kDa protein 6, chloroplastic | Q9STW6 | At4g24280 | TMS | 51 (31) | 813 | 67.2/4.79 | 63.8/4.89 | 4.3 | 6.9 |
| 22 | Heat shock 70 kDa protein 6, chloroplastic | Q9STW6 | At4g24280 | TMS | 51 (31) | 795 | 67.2/4.79 | 64.0/4.90 | 3.2 | 2.9 |
| 23 | Heat shock 70 kDa protein 6, chloroplastic | Q9STW6 | At4g24280 | TMS | 51 (31) | 889 | 67.2/4.79 | 63.9/4.92 | 2.0 | 2.2 |
| 24 | Heat shock 70 kDa protein 6, chloroplastic | Q9STW6 | At4g24280 | TMS | 51 (31) | 609 | 67.2/4.79 | 64.0/4.93 | 4.1 | 2.8 |
| 25 | Elongation factor Tu, chloroplastic | P17745 | At4g20360 | PMF | 36 (13) | 154 | 44.7/5.31 | 42.4/5.53 | 2.5 | 2.7 |
| 26 | Actin-8 | Q96293 | At1g49240 | PMF | 30 (7) | 136 | 41.9/5.37 | 41.9/5.56 | 2.4 | 0.3 |
| 27 | Oxygen-evolving enhancer protein 1-1, chloroplastic | P23321 | At5g66570 | PMF | 43 (10) | 185 | 26.6/4.93 | 26.5/5.08 | — | 0.3 |
| 28 | Oxygen-evolving enhancer protein 1-1, chloroplastic | P23321 | At5g66570 | PMF | 43 (10) | 185 | 26.6/4.93 | 26.2/5.15 | — | 0.4 |
| 29 | Triosophosphate isomerase, cytosolic | P48491 | At3g55440 | PMF | 61(9) | 150 | 27.2/5.39 | 25.6/5.57 | — | 0.4 |
| 30 | Glutathione S-transferase F10 | P42761 | At2g30870 | TMS | 33 (7) | 456 | 24.1/5.49 | 24.1/5.65 | 2.1 | 2.2 |
| 31 | 20 kDa chaperonin, chloroplastic | O65282 | At5g20720 | TMS | 72 (10) | 623 | 21.4/5.23 | 24.2/5.51 | 2.0 | 3.5 |
| 32 | Heat shock 70 kDa protein 10, mitochondrial | Q9LDZ0 | At5g09590 | TMS | 17 (10) | 238 | 68.8/5.14 | 54.8/4.99 | — | 4.5 |
| 33 | Ribulose bisphosphate carboxylase large chain (fragment) | O03042 | AtCg00490 | PMF | 60 (31) | 233 | 52.7/5.88 | 25.0/5.80 | 2.1 | — |
| 34 | Uncharacterized protein At1g13930/F16A14.27 | Q9XI93 | At1g13930 | PMF | 27 (10) | 171 | 16.2/4.82 | 10.5/5.36 | 13.6 | 8.2 |
| 35 | Translationally-controlled tumor protein homolog | P31265 | At3g16640 | TMS | 27 (4) | 403 | 18.9/4.52 | 16.3/4.75 | 2.0 | 2.7 |
| 36 | Thioredoxin M4, chloroplastic | Q9SEU6 | At3g15360 | TMS | 16 (3) | 253 | 12.5/5.42 | 13.2/4.98 | 0.3 | 0.1 |
| 37 | Annexin D1 | Q9SYT0 | At1g35720 | TMS | 19 (4) | 248 | 36.2/5.21 | 35.5/5.93 | 0.3 | 0.4 |
| 38 | Glyceraldehyde-3-phosphate dehydrogenase A, chloroplastic | P25856 | At3g26650 | PMF | 14 (5) | 91 | 36.3/6.67 | 37.5/6.58 | — | 3.2 |
| 39 | Cell division control protein 48 homolog A | P54609 | At3g09840 | TMS | 8 (5) | 188 | 89.3/5.13 | 63.9/5.52 | — | — |
| 40 | Mediator of RNA polymerase II transcription subunit 37a | Q9LKR3 | At5g28540 | PMF | 26 (17) | 149 | 70.8/5.05 | 54.7/5.52 | — | — |

**Table 1** (*continued*)

| Spot | Protein name | UniProt accession | TAIR accession | ID method | Sequence cov% (peptides) | ID score | Theor. $M_r$ (kDa)/p*I* | Exp. $M_r$ (kDa)/p*I* | Relative fold change *vs.* control | |
|---|---|---|---|---|---|---|---|---|---|---|
| | | | | | | | | | Cold | Heat |
| 41 | Mediator of RNA polymerase II transcription subunit 37f | Q39043 | At5g42020 | TMS | 24 (14) | 668 | 71.1/5.08 | 54.8/5.43 | — | — |
| 42 | Ribulose bisphosphate carboxylase large chain | O03042 | AtCg00490 | TMS | 11 (6) | 91 | 52.7/5.88 | 52.1/5.44 | — | — |
| 43 | Ribulose bisphosphate carboxylase large chain | O03042 | AtCg00490 | TMS | 26 (12) | 161 | 52.7/5.88 | 52.0/5.51 | — | — |
| 44 | Ribulose bisphosphate carboxylase large chain | O03042 | AtCg00490 | TMS | 20 (9) | 415 | 52.7/5.88 | 51.9/5.57 | — | — |
| 45 | ATP synthase subunit beta, chloroplastic | P19366 | AtCg00480 | TMS | 34 (12) | 91 | 53.9/5.38 | 52.0/5.63 | — | — |
| 46 | Ribulose bisphosphate carboxylase large chain | O03042 | AtCg00490 | TMS | 16 (7) | 91 | 52.7/5.88 | 51.9/5.78 | — | — |
| 47 | Ribulose bisphosphate carboxylase large chain | O03042 | AtCg00490 | PMF | 28 (21) | 161 | 52.7/5.88 | 51.8/5.89 | — | — |
| 48 | Ribulose bisphosphate carboxylase large chain | O03042 | AtCg00490 | TMS | 23 (9) | 1441 | 52.7/5.88 | 51.7/6.30 | — | — |
| 49 | ATP synthase subunit beta, chloroplastic | P19366 | AtCg00480 | PMF | 11 (3) | 269 | 53.9/5.38 | 52.1/4.74 | — | — |
| 50 | Protein disulfide-isomerase like 2-1 | O22263 | At2g47470 | TMS | 34 (10) | 475 | 37.1/5.65 | 41.9/5.66 | — | — |
| 51 | Cysteine synthase, chloroplastic/chromoplastic | P47999 | At2g43750 | PMF | 25 (7) | 554 | 35.1/5.54 | 39.8/5.74 | — | — |
| 52 | Ribulose bisphosphate carboxylase/oxygenase activase, chloroplastic | P10896-2 | At2g39730 | PMF | 30 (16) | 169 | 43.4/5.42 | 39.8/5.43 | — | — |
| 53 | Ribulose bisphosphate carboxylase/oxygenase activase, chloroplastic | P10896-2 | At2g39730 | PMF | 37 (15) | 186 | 43.4/5.42 | 39.8/5.53 | — | — |
| 54 | Ribulose bisphosphate carboxylase/oxygenase activase, chloroplastic | P10896-2 | At2g39730 | PMF | 32 (17) | 188 | 43.4/5.42 | 39.5/5.58 | — | — |
| 55 | Malate dehydrogenase 1, mitochondrial | Q9ZP06 | At1g53240 | PMF | 42 (9) | 741 | 33.3/6.00 | 35.5/6.70 | — | — |
| 56 | Malate dehydrogenase 1, mitochondrial | Q9ZP06 | At1g53240 | TMS | 26 (9) | 643 | 33.3/6.00 | 35.5/6.45 | — | — |
| | Eukaryotic translation initiation factor 2 subunit beta | Q41969 | At5g20920 | TMS | 10 (3) | 110 | 30.7/6.79 | | — | — |
| 57 | Ribulose bisphosphate carboxylase/oxygenase activase, chloroplastic (fragment) | P10896 | At2g39730 | PMF | 16 (8) | 114 | 46.2/5.09 | 26.5/5.15 | — | — |
| 58 | Oxygen-evolving enhancer protein 1-2, chloroplastic | Q9S841 | At3g50820 | TMS | 49 (14) | 1154 | 26.6/5.02 | 26.2/5.25 | — | — |
| 59 | Carbonic anhydrase, chloroplastic | P27140 | At3g01500 | PMF | 39 (12) | 202 | 25.6/6.14 | 21.9/5.53 | — | — |
| 60 | Ribulose bisphosphate carboxylase small chain 3B, chloroplastic | P10798 | At5g38410 | PMF | 47 (9) | 184 | 14.8/5.71 | 10.5/6.25 | — | — |
| 61 | Ribulose bisphosphate carboxylase small chain 3B, chloroplastic | P10798 | At5g38410 | PMF | 52 (10) | 199 | 14.8/5.71 | 8.3/6.25 | — | — |
| 62 | Ribulose bisphosphate carboxylase small chain 3B, chloroplastic | P10798 | At5g38410 | PMF | 43 (8) | 152 | 14.8/5.71 | 8.3/6.52 | — | — |

from MALDI-TOF PMF data, whereas 18 from nanoLC-ESI-LIT-MS/MS ones; two spots were associated with multiple proteins and were not further discussed. Globally, spots assayed were associated with 28 non-redundant protein entries. The list of identified protein species, together with their quantitative variations as a result of cold and heat shock treatments, is reported in Table 1. Some proteins, such as heat shock 70 kDa protein 6, ribulose bisphosphate carboxylase large and small 2B subunits, 29 kDa ribonucleoprotein (CP29A) and oxygen-evolving enhancer proteins 1-1 and 2-1, occurred as multiple spots whose structural differences were not further characterized. Ribulose bisphosphate carboxylase large chain and ribulose bisphosphate carboxylase/oxygenase activase were also identified among constant spots (see below). Probably, they were the result of post-translational modification or differential splicing events. Functional categorization according to Gene Ontology annotation and literature data (data not shown) showed that differentially-represented proteins grouped into two main broad classes including components involved in energy and metabolism (55%) or in stress response (34%); the remaining proteins (11%) were related to different processes and were categorized as a miscellaneous group.

A Venn diagram representation of the differentially-represented spots indicated that a significant overlap occurred between the response to short-term cold and heat shock (Fig. 3). In fact, quantitative levels of 25 protein spots were affected by both temperature treatments. In particular, 10 proteins, namely ribulose bisphosphate (RuBis) carboxylase/oxygenase activase (spot 3), heat shock 70 kDa protein (HSP70) 6 (spots 21–24), elongation factor Tu (EF-Tu) (spot 25), glutathione *S*-transferase (GST) F10 (spot 30), 20 kDa chaperonin (spot 31), uncharacterized

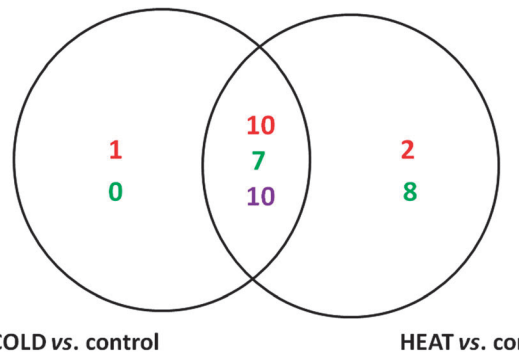


**Fig. 3** Venn diagram analysis of the differentially expressed proteins during cold or heat shock treatments. Twenty-five protein spots were affected by both temperature treatments, 23 protein spots were differentially-represented following treatments, whereas 2 protein spots were detected only in control samples. Red, over-represented spots; green, down-represented spots; purple, over-represented spots in cold *vs.* control and down-represented in heat *vs.* control.

 

protein At1g13930/F16A14.27 (spot 34) and translationally-controlled tumor protein (TCTP) homolog (spot 35) were over-represented following both cold and heat stress; five proteins, namely chloroplast stem-loop binding protein of 41 kDa (spot 8), germin-like protein subfamily member 3 (spot 16), peptidyl-prolyl *cis–trans* isomerase CYP20-3 (CYP20-3) (spot 17), thioredoxin (TRX) M4 (spot 36) and annexin (ANX) D1 (spot 37), together with those comigrating in spots 5 and 20, were down-represented or absent following both cold and heat stress; ten protein spots, namely RuBis carboxylase large chain (spots 1 and 2), magnesium chelatase subunit ChlI-1 (spot 4), fructose-bisphosphate aldolase 2 (spot 6), ATP synthase (ATPase) gamma chain 1 (spot 7), 29 kDa ribonucleoprotein (spot 11), oxygen-evolving enhancer (OEE) protein 2–1 (spot 14), RuBis carboxylase small chain 2B (spots 18 and 19) and actin 8 (spot 26) were over-represented after cold shock and down-represented following heat shock.

On the other hand, a number of highly represented protein spots were recognized as constantly present within the different 2-DE maps. Among that, 24 (spots 39–62) were similarly sampled from gels, trypsinolyzed and subjected to MS analysis for protein identification; all spots were associated with a unique protein sequence entry, with a unique exception (spot 56) in which multiple components migrated together (Table 1). Constant spots were identified as RuBis carboxylase small chain 3B, ATPase subunit beta, protein disulfide-isomerase like 2-1, cysteine synthase, malate dehydrogenase 1, eukaryotic translation initiation factor 2 subunit beta, OEE protein 1-2, carbonic anhydrase, cell division control protein 48 homolog A, and mediator of RNA polymerase II transcription subunits 37a and 37f, as well as specific isoforms of RuBis carboxylase large chain and RuBis carboxylase/oxygenase activase.

### 3.3 Proteins affected by cold treatment

Proteomic analysis suggested that short-term cold treatment of *Arabidopsis thaliana* had a significant effect on specific processes of plant photosynthesis. In fact, incubation of seedlings at 4 °C, for 6 h, brought about a quantitative increase in proteins involved both in electron transport/energy production and carbon metabolism reactions or, at least, specific isoforms of them. As far as the first protein family, ATPase gamma chain (spot 7), and isoforms of OEE protein 2-1 (spot 14) and of 29 kDa chloroplastic ribonucleoprotein (spot 11) were up-regulated, respectively. Among Calvin cycle enzymes, levels of RuBis carboxylase small chain 2B (spots 18 and 19) and of specific isoforms of RuBis carboxylase large chain (spots 1, 2 and 33) and RuBis carboxylase/activase (spot 3) were significantly increased. On the other hand, ATPase beta chain, OEE proteins 1-1 and 1-2, photosystem I reaction center subunit II-2, RuBis carboxylase small chain 3B, and other isoforms of RuBis carboxylase large chain and RuBis carboxylase/oxygenase activase remained constantly represented.

On the overall, the observed trends are fairly in accordance with previous literature data. In fact, increased abundance of specific components of the thylakoid photosynthetic apparatus, including OEE proteins, has been already observed in cold-treated *Arabidopsis*[10] or in the cold-tolerant species *Thellungiella halophila* subjected to short-term cold challenge.[15] Similarly, increased levels of certain chloroplast electron transport chain components have been related to improved cold resistance.[32] As far as CP29A, our findings point to a pivotal role of this protein in cold tolerance. In fact, it has been identified by previous proteomic investigations as a cold up-regulated species both in *Arabidospsis*[10] and *Thellungiella,*[15] while differences in CP29A phosphorylation status have been reported between cold-tolerant and sensitive maize cultivars, and correlated to photoinhibition of cold-sensitive lines.[33] In *Arabidopsis*, it has recently been shown that CP29A and CP31A are essential to maintain transcript stability of different chloroplast mRNAs under cold stress.[34] Conversely, contrasting data have been reported for the effect of cold stress on the abundance of Calvin cycle enzymes, depending on the species investigated and/or the type of cold treatment.[14] For example, increased levels of RuBis carboxylase large subunit have been reported in rice, together with extensive protein degradation,[13] whereas a heterogeneous pattern was observed in *Thellungiella*, depending on time of treatment and spot multiplicity.[15] The latter scenario may result from the occurrence of post-translational modifications (*i.e.* phosphorylation, sumoylation) that can affect electron transport/energy production and carbon metabolism enzymes under stress conditions.[35,36] Their detection needs dedicated approaches to ascertain the presence of specific isoforms in 2-DE maps, as we detected in this study. Under our conditions, the stress treatment caused a significant increase in the abundance of RuBis carboxylase small chain 2B (spots 18 and 19) and of specific isoforms of both RuBis carboxylase large chain and RuBis carboxylase/oxygenase activase; proteolytic degradation of RuBis carboxylase large chain was also observed. Finally, cold stress has been reported to determine an up-regulation of carbon catabolism enzymes.[14] In this context, we identified only fructose-bisphosphate aldolase 2 as up-regulated enzyme. This protein is involved in chloroplast glycolysis, and its levels have been reported to increase in rice leaves in response to long-term (48 h) cold stress.[13]

The second prominent functional group was represented by proteins involved in the response to environmental stresses. In particular, an over-representation of four spots (21, 22, 23 and 24) associated with 70 kDa class of heat shock protein 6 was evident following cold shock. Their electrophoretic pattern suggests that, notwithstanding the occurrence of post-translational modifications affecting corresponding polypeptide chain, increased amounts of all protein isoforms were detected. Quantitative levels of 20 kDa chaperonin (spot 31) and GST F10 (spot 30) were also significantly increased, while those of protein At1g13930/F16A14.27 (spot 34), an uncharacterized component ''involved in salt stress response'', showed the largest increase among up-regulated components.

HSP70s belong to a conserved family of molecular chaperones that assist folding, assembly, translocation and degradation of proteins in all cellular compartments. By stabilizing protein conformation, they are essential to maintain cellular homeostasis under stressing conditions;[37] their increase in response to a wide range of environmental stresses (including cold) has been reported in different plant species.[14] Interestingly, HSP70s have been reported in *Arabidopsis* as nuclear proteins induced after

short-term cold challenge.[8] 20 kDa chaperonin is chloroplast-located and its induction, which in this study parallels to that of many other chloroplastic polypeptides (34% of deregulated components concerned chloroplast-located species), confirms the importance of this organelle in temperature stress response. Cold stress alters cellular redox homeostasis, hence it is not surprising that accumulation of different enzymes deputed to ROS neutralization has been reported in many plants,[14] including components of the ascorbate–glutathione cycle and various GST isoforms.[14,32,38] Here, we identified a member of the phi class of the GST family, which appears to be ubiquitous in plant tissues and whose down-regulation in transgenic plants causes reduced tolerance to abiotic stresses.[39] Indeed, At1g13930 was previously identified by means of a functional gene-mining method to isolate salt stress tolerance genes in *Thellungiella halofila.*[40] Its function is unknown but it has been associated with salt tolerance; its strong up-regulation in our conditions suggests that it can also play a key role in cold tolerance.

On the other hand, the abundance of chloroplastic TRX M4 (spot 36), chloroplastic CYP20-3 (spot 17), ANX D1 (spot 37) and germin-like protein 3 (spot 16) was decreased after short-term cold stress. Thioredoxins m-type have been proposed to specifically regulate chloroplast glucose-6-phosphate dehydrogenase, inhibiting in the light oxidative generation of NADPH, when it is produced by the photosynthetic electron flow.[41] Decreased levels under cold stress may reflect the necessity of the cell to increase reducing power with the aim of contrasting oxidative stress; this observation is in accordance with the general increase of glycolytic catabolic reactions detected during cold stress.[14] CYP20-3 belongs to the large family of cyclophillins, whose primary function is to assist protein folding; they are induced in response to both abiotic and biotic stresses.[24] On the other hand, annexins are a conserved family of eukaryotic $Ca^{2+}$-dependent phospholipid-binding proteins; although their expression pattern is developmentally regulated, different lines of evidence indicate that they are also involved in the protection from biotic and abiotic stresses.[42] The rationale for the observed down-regulation under our conditions of the latter two proteins is unclear at present. Indeed, germins, which belong to the conserved cupin superfamily, have been described in barley as pathogenesis-related proteins. By eliciting an oxalate oxidase or superoxide dismutase activity, they are able to generate $H_2O_2$; they are very likely involved in cell wall stiffening or signalling against pathogen infection. Germin-like genes are activated also in response to abiotic stress, such as high salinity or heat.[43] Intriguingly, germins have already been identified in *Arabidospsis* leaves as nuclear proteins down-regulated upon short-term cold challenge.[8]

Other variably-represented proteins were identified as components whose function was related to various cellular processes; they included actin 8 (spot 26), TCTP homolog (spot 35), EF-Tu (spot 25) and magnesium-chelatase subunit ChlI-1 (CHLI) (spot 4). The first two proteins are structural components involved in cytoskeleton organization and stabilization, respectively. Plasma membrane is an early target of cold injury and experimental evidence suggests that actin filaments of the cytoskeleton, as linked to the plasma membrane, are involved in the sensing of and in the response to low temperature.[44] In the moss *Psyscomitrella patens*, cellular actin content dramatically increases after long term cold stress.[45] Under our conditions, actin and TCTP homolog increased as well, even at much shorter times of cold exposure, although to a lesser extent. These findings reinforce the idea that cytoskeleton is an early target of cold damage; its rearrangement may play a pivotal role in cold tolerance. On the other hand, EF-Tu and CHLI are chloroplast-located proteins involved in the regulation of plastidial protein synthesis and chlorophyll biosynthesis, respectively; under our conditions, both proteins were up-regulated after cold stress. An EF-Tu over-representation has been already reported in cytokinin over-expressing creeping bentgrass under drought conditions;[46] it was paralleled by an increase of chloroplastic enzymes involved in photosynthesis and energy production. Our results also point to a role for this protein in sustaining protein synthesis within the chloroplast, in order to preserve the integrity of the energy production machinery under cold stress conditions. As far as magnesium-chelatase is concerned, it is worth mentioning that different subunits (CHLH, CHLI) of this enzyme have recently been shown to be involved in abscisic acid (ABA) signaling modulation.[47] ABA is a well-known environment-responsive phytohormone that plays a key role in adaptation to different stresses, including the cold one.[48]

### 3.4 Proteins affected by heat treatment

Short-term heat treatment (42 °C, 6 h) of *Arabidopsis* seedlings also affected the abundance of leaf proteins involved in the photosynthetic electron transport and carbon metabolism. Unlikely to cold stress, a general protein down-representation was observed in this case. In fact, levels of OEE protein 2-1 (spots 14 and 15), OEE protein 1-1 (spots 27 and 28), subunit II-2 of the photosystem I reaction center (spots 9 and 13) and chloroplastic 29 kDa ribonucleoprotein (spots 11 and 12) were significantly reduced; the same trend was also observed for RuBis carboxylase small chain 2B (spots 18 and 19) and specific isoforms of RuBis carboxylase large chain (spots 1 and 2). Similarly to cold stress, a consistent increase of a specific isoform of RuBis carboxylase/oxygenase activase was conversely detected (spot 3). On the other hand, RuBis carboxylase small chain 3B, and other isoforms of RuBis carboxylase large chain and RuBis carboxylase/oxygenase activase remained constantly represented. Indeed, heat stress was shown to down-regulate different key enzymes of the Calvin cycle in rice, including RuBis carboxylase,[49] while an up-regulation of RuBis carboxylase/oxygenase activase has already been reported in rice[49] and wheat.[50] It has been suggested that a RuBis carboxylase/oxygenase activase over-representation may be part of the adaptative response, in order to maintain $CO_2$ fixation under stress conditions.[22] Considerations analogous to that reported above for cold stress can be formulated to justify the isoform-specific pattern of electron transport/energy production and carbon metabolism enzymes as a result of post-translational modifications.[35,36]

As far as carbon metabolism and energy generation, it has been shown that heat stress negatively affects the glycolytic

 

pathway and reduces energy production in rice, bringing about a marked decrease in the levels of different glycolytic enzymes or proteins involved in energy-generating reactions.[23] In agreement with this scenario, we observed a down-representation of fructose-bisphosphate aldolase 2 (spot 6), cytosolic triosephosphate isomerase (spot 29), ATPase gamma chain (spot 7) and soluble inorganic pyrophosphatase 1 (PPase1) (spot 10), whereas an increase in the abundance of chloroplastic glyceraldehyde 3-phosphate dehydrogenase (GAPDH) (spot 38) was detected. By catalyzing the exergonic hydrolysis of pyrophosphate, PPase1 plays a crucial role in cellular energy conservation. On the other hand, plants contain three forms of GAPDH encoded by distinct genes: a cytosolic form that participates in glycolysis and two chloroplast forms involved in photosynthesis. It has been suggested that glycolytic GAPDH may be also involved in stress response, since its levels are increased by different environmental challenges, including heat;[23] no literature data are available on stress modulation of chloroplastic GAPDH.

Similarly to cold stress, the second functional group most influenced by heat treatment was that of proteins involved in stress response, particularly molecular chaperones. In fact, heat stress is primarily associated with improper protein folding or denaturation. Likewise cold stress, four spots (21, 22, 23 and 24) identified as 70 kDa class of heat shock protein 6 were consistently up-regulated, together with another strongly induced mitochondrial HSP70, *i.e.* isoform 10 (spot 32), apparently specific for the heat stress condition. Finally, levels of 20 kDa chaperonin (spot 31) were more prominently up-regulated than in cold stress, while that of CYP20-3 (spot 17) were similarly decreased. A general deregulation of proteins with a protecting role from oxidative damage was also observed in this case, with a pattern similar to that induced by cold stress. In fact, GST F10 (spot 30) was over-represented, while levels of chloroplastic TRX M4 (spot 36) were decreased. Among other proteins involved in stress response, worth noting is that uncharacterized protein At1g13930/F16A14.27 (spot 34) was the most prominently over-represented component, as in the case of cold stress; this suggests a general role for this protein in adaptation to fast temperature changes. On the other hand, ANX D1 (spot 37) and germin-like protein 3 (spot 16) were both down-regulated, similarly to cold stress.

As far as proteins involved in other cellular functions, the pattern of expression following heat stress was qualitatively reminiscent of that resulting from cold stress, concerning a limited number of components involved in similar functions. Cytoskeleton structure was apparently a target also for heat stress injury. Microtubule stabilizer TCTP homolog (spot 35) was up-regulated after heat shock, analogously to cold stress, while actin 8 (spot 26) was down-regulated. Finally, EF-Tu (spot 25) abundance was increased to the same extent as under low temperature conditions. Besides promoting aminoacyl-tRNA binding to ribosomes, it has been reported that this protein can function as a molecular chaperone under heat stress conditions, thus protecting chloroplast proteins from misfolding and aggregation;[51] accordingly, its synthesis is differentially regulated in heat-sensitive and tolerant maize cultivars.[52]

## 4 Concluding remarks

Proteomics can significantly contribute to the understanding of physiological modifications underlying response of plants to temperatures stresses, which generally involves profound changes in the cellular protein repertoire.[14] Proteomic information on plant temperature stress is still fragmentary, mostly concerning the study of adaptative responses of crop species. Since stress response is influenced by duration and intensity of temperature challenge (*i.e* shock or adaptation), corresponding patterns of proteome variations are expected to be (very likely) only partially coincident. Here we have reported on the comparative proteomic analysis of the effect of short-term cold and heat treatment (shock) on leaves of the model species *Arabidopsis thaliana*. Results allowed us to identify a number of proteins, participating in different cellular functions, some of which are already known to be involved in response to prolonged cold or heat stresses or acclimation in *Arabidopsis* and/or other species.[14,15,23] Novel proteins were also identified as potential markers to be associated with the alteration of cellular functions imposed by temperature stress or to the acquisition of stress tolerance. In this context, original information was derived for At1g13930/F16A14.27, CHL1, EF-Tu, chloroplastic GAPDH, TCTP, chloroplastic TRX M4, GST F10, chloroplastic 20 kDa chaperonin and mitochondrial HSP70 isoform 10. On the other hand, data on the remaining differentially-represented proteins corroborate previous observations on temperature treatments under various experimental conditions in *Arabidopsis, Thellungiella*, maize or rice.[10,13,15,33,34,52]

Our experiments ascertained that a significant degree of overlapping exists between metabolic alterations induced by, and/or in response to cold and heat short-term challenge. In fact, many differentially-represented proteins were modulated by both stimuli, with some remarkable exceptions, from which specific features of cold or heat responses can be inferred. According to literature data, chloroplast and also plasma membrane/cytoskeleton were confirmed as early targets for temperature injury. Cold and heat influenced photosynthesis in opposition. Over-representation of enzymes involved in electron transport and Calvin cycle seems to be distinctive of the cold response, aimed at protection of plant from photoinhibition. This response is apparently hampered by heat stress, which probably affects thylakoidal structures more severely; on the other hand, the shared proteomic signatures we observed may be part of a common cellular strategy to sustain carbon fixation under general stress conditions. In this context, 29 kDa ribonucleoprotein (specifically induced by cold stress) may deserve supplemental studies to envisage its possible use as a marker for cold tolerance selection. On the other hand, CHLI, chloroplastic GAPDH and uncharacterized protein At1g13930/F16A14.27 emerged as novel intriguing chloroplast proteins, induced by cold, heat stress or both, respectively, which could also be investigated for their possible use as temperature tolerance markers. Our results also confirmed that major components of the early response to temperature stress are HSPs. Among the different chaperones whose increase has

been reported in different species, HSP70 isoform 10 and 20 kDa chaperonin were here preferentially induced either following heat and cold stresses, while the HSP70 isoform 10 was apparently specific to the heat shock condition. Finally, cytoplasmic detoxification of ROS relied preferentially on the induction of GST under both cold or heat stress. In conclusion, our investigation corroborates previous observations of quantitative proteomic changes in other species and defines a more focused picture of the early protein changes associated with both temperature challenges, which can hopefully orient future integrated approaches to gain a deeper insight into the complex network of plant response to environmental stresses.



## Acknowledgements

This study was partially supported by grants from the Italian Ministry of Economy and Finance (Progetto Innovazione e Sviluppo del Mezzogiorno – Conoscenze Integrate per Sostenibilità ed Innovazione del Made in Italy Agroalimentare'' – Legge n. 191/2009).

## References

1 J. Levitt, *Responses of plants to environmental stress*, Academic Press, New York, USA, 2nd edn, 1980.
2 J. Kilian, F. Peschke, K. W. Berendzen, K. Harter and D. Wanke, *Biochim. Biophys. Acta*, 2012, **1819**, 166–175.
3 A. R. Fernie and M. Stitt, *Plant Physiol.*, 2012, **158**, 1139–1145.
4 N. P. A. Huner, G. Öquist, V. M. Krol, S. Falk and M. Griffith, *Photosynth. Res.*, 1993, **37**, 19–39.
5 K. Yamaguchi-Shinozaki and K. Shinozaki, *Annu. Rev. Plant Biol.*, 2006, **57**, 781–803.
6 V. Chinnusamy, J. Zhu and J. K. Zhu, *Trends Plant Sci.*, 2007, **12**, 444–451.
7 J. Zhu, H. Shi, B. H. Lee, B. Damsz, S. Cheng, V. Stirm, J. K. Zhu, P. M. Hasegawa and R. A. Bressan, *Proc. Natl. Acad. Sci. U. S. A.*, 2004, **101**, 9873–9878.
8 M. S. Bae, E. J. Cho, E. Y. Choi and O. K. Park, *Plant J.*, 2003, **36**, 652–663.
9 Y. Kawamura and M. Uemura, *Plant J.*, 2003, **36**, 141–154.
10 S. Amme, A. Matros, B. Schlesier and H. P. Mock, *J. Exp. Bot.*, 2006, **57**, 1537–1546.
11 T. Li, S. L. Xu, J. A. Oses-Prieto, S. Putil, R. J. Wang, K. H. Li, D. A. Maltby, L. H. An, A. L. Burlingame, Z. P. Deng and Z. Y. Wang, *Mol. Plant*, 2011, **4**, 361–374.
12 S. P. Yan, Q. Y. Zhang, Z. C. Tang, W. A. Zu and W. N. Sun, *Mol. Cell. Proteomics*, 2006, **5**, 484–496.
13 M. Hashimoto and S. Komatsu, *Proteomics*, 2007, **7**, 1293–1302.
14 K. Kosova, P. Vitamvas, I. T. Prasil and J. Renautt, *J. Proteomics*, 2011, **74**, 1301–1322.
15 F. Gao, Y. Zhou, W. Zhu, X. Li, L. Fan and G. Zhang, *Planta*, 2009, **230**, 1033–1046.
16 E. Goulas, M. Schubert, T. Kieselbach, L. A. Kleczkowski, P. Gardestrom, W. Schoeder and V. Hurry, *Plant J.*, 2006, **47**, 720–734.
17 R. Mittler, A. Finka and P. Goloubinoff, *Trends Biochem. Sci.*, 2012, **37**, 118–125.
18 D. Quin, H. Wu, H. Peng, Y. Yao, Z. Ni, Z. Li, C. Zhou and Q. Sun, *BMC Genomics*, 2008, **9**, 432.
19 N. Suzuki, S. Bajad, J. Shuman, V. Shulaev and R. Mittler, *J. Biol. Chem.*, 2008, **283**, 9269–9275.
20 K. A. Neilson, C. G. Gammulla, M. Mirzaei, N. Limin and P. A. Haynes, *Proteomics*, 2010, **10**, 828–845.
21 M. Palmblad, D. J. Mills and L. V. Bindschedler, *J. Proteome Res.*, 2008, **7**, 780–785.
22 J. Zou, C. Cuifang and X. Chen, *Plant Cell Rep.*, 2011, **30**, 2155–2165.
23 D. G. Lee, N. Ashan, S. H. Lee, K. Y. Kang, J. D. Bahk, I. J. Lee and B. H. Lee, *Proteomics*, 2007, **7**, 3369–3383.
24 C. Huang, F. Verrillo, G. Renzone, S. Arena, M. Rocco, A. Scaloni and M. Marra, *J. Proteomics*, 2011, **74**, 1934–1949.
25 S. P. Yan, Q. Y. Zhang, Z. C. Tang, W. A. Wu and W. N. Sun, *Mol. Cell. Proteomics*, 2006, **5**, 484–496.
26 M. Rocco, C. D'Ambrosio, S. Arena, M. Faurobert, A. Scaloni and M. Marra, *Proteomics*, 2006, **6**, 3781–3791.
27 L. S. Ramagli and L. V. Rodriguez, *Electrophoresis*, 1985, **6**, 559–563.
28 F. Talamo, C. D'Ambrosio, S. Arena, P. Del Vecchio, L. Ledda, G. Zehender, L. Ferrara and A. Scaloni, *Proteomics*, 2003, **3**, 440–460.
29 G. Bernardini, G. Renzone, M. Comanducci, R. Mini, S. Arena, C. D'Ambrosio, S. Bambini, L. Trabalzini, G. Grandi, P. Martelli, M. Achtman, A. Scaloni, G. Ratti and A. Santucci, *Proteomics*, 2004, **4**, 2893–2926.
30 G. S. Scippa, M. Rocco, M. Ialicicco, D. Trupiano, V. Viscosi, M. Di Michele, S. Arena, D. Chiatante and A. Scaloni, *Electrophoresis*, 2010, **31**, 497–506.
31 W. J. Qian, T. Li, M. E. Monroe, E. F. Strittmatter, J. M. Jacobs, L. J. Kangas, K. Petrits, D. G. Camp 2nd and R. D. Smith, *J. Proteome Res.*, 2005, **4**, 53–62.
32 A. Kosmala, A. Bocian, M. Rapacz, B. Jurczyk and Z. Zwierzykowsi, *J. Exp. Bot.*, 2009, **60**, 3595–3609.
33 S. Mauro, P. Dainese, R. Lannoye and R. Bassi, *Plant Physiol.*, 1997, **115**, 171–180.
34 C. Kupsc, H. Ruwe, S. Gusewski, M. Tillich, I. Small and C. Schmitz-Linneweber, *Plant Cell*, 2012, **24**, 4266–4280.
35 S. J. Hey, E. Byrne and N. G. Halford, *Ann. Bot.*, 2010, **105**, 197–203.
36 P. H. Castro, R. M. Tavares, E. R. Bejarano and H. Azevedo, *Cell. Mol. Life Sci.*, 2012, **69**, 3269–3283.
37 W. Wang, B. Vinocur, O. Shoseyov and A. Altman, *Trends Plant Sci.*, 2004, **9**, 244–252.
38 Y. Kawamura and M. Uemara, *Plant J.*, 2003, **36**, 141–154.
39 H. Y. Ryu, S. Y. Kim, H. M. Park, J. Y. You, B. H. Kim, J. S. Lee and K. H. Nama, *Biochem. Biophys. Res. Commun.*, 2009, **379**, 417–422.
40 J. Du, Y. P. Huang, J. Xi, M. J. Cao, W. S. Ni, X. Chen, J. K. Zhu, D. J. Oliver and C. B. Xiang, *Plant J.*, 2008, **56**, 653–664.
41 G. Née, M. Zaffagnini, P. Trost and E. Issakidis-Bourget, *FEBS Lett.*, 2009, **583**, 2827–2832.

 

42 S. K. Jami, G. B. Clark, B. T. Ayele, P. Ashe and P. B. Kirti, *PLoS One*, 2012, **7**, 1–14.
43 A. Himmelbach, L. Liu, L. Altschmied, H. Maucher, F. Beier, D. Müller, G. Hensel, A. Heise, A. Schützendübel, J. Kumlehn and P. Schweizer, *Plant Cell*, 2010, **22**, 937–952.
44 B. L. Orvar, V. Sangwan, J. Singh and R. S. Dhindsa, *Plant J.*, 2000, **23**, 788–794.
45 X. Wang, P. Yang, X. Zhang, Y. Xu, T. Kuang, S. Shen and Y. He, *Proteomics*, 2009, **9**, 4529–4538.
46 E. B. Merewtz, T. Gianfagna and B. Huang, *J. Exp. Bot.*, 2011, **62**, 5311–5333.
47 S. Y. Du, X. F. Zhang, Z. Lu, Q. Xin, Z. Wu, T. Jiang, Y. Lu, X. F. Wang and D. P. Zhang, *Plant Mol. Biol.*, 2012, **80**, 519–537.
48 V. Chinnusamy, K. Schumaker and J. K. Zhu, *J. Exp. Bot.*, 2004, **55**, 225–236.
49 F. Hang, H. Chen, X. J. Lin, M. F. Yang, G. S. Liu and S. H. Shen, *Biochim. Biophys. Acta*, 2009, **1794**, 1625–1634.
50 R. D. Law and S. J. Craft-Brandner, *Arch. Biochem. Biophys.*, 2001, **386**, 261–267.
51 D. Rao, I. Momcilovic, S. Kobayashi, E. Callegari and Z. Ristic, *Eur. J. Biochem.*, 2004, **27**, 13684–13692.
52 I. Momcilovic and Z. Ristic, *J. Plant Physiol.*, 2007, **164**, 90–99.